ELSEVIER

Journal of Archaeological Science 32 (2005) 1053–1060

Journal of Archaeological SCIENCE

http://www.elsevier.com/locate/jas

Post-mortem DNA damage hotspots in Bison (*Bison bison*) provide evidence for both damage and mutational hotspots in human mitochondrial DNA

M.T.P. Gilbert[a,*], B. Shapiro[a], A. Drummond[b], A. Cooper[a,1]

[a] *Henry Wellcome Ancient Biomolecules Centre, Department of Zoology, University of Oxford, South Parks Road, Oxford OX1 3PS, UK*

[b] *Department of Zoology, University of Oxford, South Parks Road, Oxford OX1 3PS, UK*

Received 24 June 2004; received in revised form 7 February 2005

Abstract

Post-mortem damage-driven mutations are a phenomena associated with ancient DNA (aDNA) studies. A previous study has demonstrated that the distribution of such mutations in human mitochondrial DNA is not random, but is concentrated in 'hotspots' that correlate with sites of elevated mutation rate in vivo. However, as the previous study was undertaken on human samples, it is possible for a critic to argue that the results might be biased through the presence of modern contaminant DNA sequences among the ancient DNA extracts. In this study we confirm the phenomena of DNA damage hotspots using a data set that is unlikely to be affected by contamination – cloned mitochondrial control region sequences extracted from 81 ancient bison (*Bison bison*). Furthermore, using published data from modern bovid specimens, we confirm that the damage hotspots correlate with sites of in vivo hypermutation. In conclusion, the aDNA sequences from archaeological specimens provide evidence that structural elements of mitochondrial DNA confer a degree of in vivo and post-mortem protection from sequence modification. This in turn provides useful insights into the debate as to whether mutational hotspots or mitochondrial recombination might best explain homoplasies observed on phylogenetic trees of human mitochondrial sequences.

Keywords: aDNA; Bison; Damage; Mitochondria; Sequence

1. Introduction

Certain nucleotide positions (termed 'sites') within the human mitochondrial genome have been reported to mutate at rates that are significantly higher than average, and have thus been described as mutational [2,4,7–9,15–17,19,22–26,29,30,32,33,35–38]. Although some of these studies have identified hotspots through the direct comparison of closely related (e.g. familial) DNA sequences [4,8,9,17,26,29,32,33], such studies are limited by the number of comparisons that can be made. This is predominantly due to the small size of available data sets, and because the rates of mitochondrial mutation are too slow to provide enough resolution to clearly distinguish individual site-specific mutational rates. For example, in a study of background radiation-induced mutations in over 980 human samples, only 22 mutations were observed over the complete mitochondrial control region hypervariable (HVR) 1 and 2 regions [9]. Therefore, in order to draw conclusions from larger data sets, most studies have estimated site-specific mutation rates using phylogenetic reconstructions of human mitochondrial

* Corresponding author. Current address: Ecology and Evolutionary Biology, University of Arizona, 1041 E. Lowell St, Tucson, AZ 85721, USA. Tel.: +1 520 621 4881; fax: +1 520 621 9190.

E-mail address: mtpgilbert@spymac.com (M.T.P. Gilbert).

[1] Current address: School of Environmental Sciences, University of Adelaide, Adelaide, SA 5005, Australia.

0305-4403/$ - see front matter © 2005 Elsevier Ltd. All rights reserved.
doi:10.1016/j.jas.2005.02.006

sequences. One weakness with this method is that the accuracy of hotspot designation is directly related to the precision of the phylogenetic model used to represent the true phylogeny. Consequently, it is not unusual for different studies to designate hotspot status for conflicting sites. One such example is the control region site 16325, identified as mutating slowly in some studies [7,25], but at above average rates when analysed with other techniques [3]. In addition to these issues, the existence of hotspots per se has also been questioned. Hagelberg has supported mitochondrial recombination, as an explanation for the homoplasies observed on phylogenetic trees that would otherwise be attributed to recurrent mutations [13].

Previous studies [11] have demonstrated that the distribution of post-mortem DNA sequence modifications (referred to as 'damage') in ancient DNA (aDNA) sequences shows strong correlation with sequence positions inferred to have elevated rates of mutation in vivo. The study suggested that DNA secondary and tertiary structure predisposes certain sites to such damage, while also protecting other sites from the same modifications [11].

Despite the stringent precautions taken by Gilbert et al. [11], all ancient human DNA studies are subject to the criticism that there is considerable potential for contamination with modern or previously amplified human DNA fragments. Contaminated samples could produce a spectrum of base variation among amplified products that would imitate sequence damage [11], and would also permit 'jumping PCR' between endogenous and contaminant strands [28]. Such 'jumping PCR' events will increase the apparent number of damaged sites in amplified sequences by introducing positions that differ between the contaminant and authentic DNA. Consequently, further investigation of post-mortem miscoding lesions requires analysis of a non-human data set where sample contamination is far less likely.

As part of the largest aDNA study to date, Shapiro et al. [31] have determined control region sequences from over 350 ancient bison (*Bison bison*) specimens. Comparable sequence data are available for modern bovids from three studies which have reported the presence of hypervariable mutational sites [6,34,40]. In this study we generate and analyze cloned PCR products from control region sequences of 81 ancient bison. We compare post-mortem damage hotspots to putative mutational hotspots in modern bison identified as homoplasies on phylogenetic trees generated from the ancient bison data set, and sites observed as hotspots (using several methods) in studies of modern bovid DNA.

2. Materials and methods

While most post-mortem DNA damage events fragment the molecule and prevent it from being amplified, a small proportion merely generates miscoding lesions [27]. These are manifested as base modifications in the amplified sequence, changing the appearance of a DNA template, and represent the basis of our analysis. The few detailed studies of miscoding lesions concur that, as in vivo, the majority of changes arise from the deamination of cytosine (C) to uracil, an analogue of thymine (T) [10,18], or the deamination of adenine (A) to hypoxanthine, an analogue of G [10]. For simplicity, both the chemical event and the phenotype are referred to hereafter simply as C → T or A → G changes. However, both of these transition events can produce two observable phenotypes depending on whether the damage event occurred on the strand that is eventually sequenced, or its' complement. For example, a C → T degradation may simply be observed as C → T, but will appear as a G → A transition if the complementary strand is sequenced. Similarly, an A → G degradation may be observed as either an A → G or a T → C transition [14,18]. Following the nomenclature of Hansen et al. [14], we term each set of miscoding lesions as type 1 (A → G/T → C) or type 2 (C → T/G → A) transitions, respectively. In addition to deamination, a small proportion of miscoding lesions may also be derived through oxidatively derived transversions [27].

Eighty-one PCR products of the bovid HVR1 region corresponding to positions 15761 − 00052 of the *Bos taurus* Reference Sequence (BtRS) (Genbank J01394 [1]) were generated and cloned from 61 ancient bison specimens. The products varied in size from 125 to 635 bp, and sequences were numbered according to a *B. bison* Reference Sequence (BbRS) for the mitochondrial light strand site (Fig. 1).

The number of PCR products generated per region of HVR1 is shown in Table 1 full details of the samples and primers are given in Shapiro et al. [31]. Strict ancient DNA procedures were used throughout, including multiple extractions from each specimen, extraction and PCR negative controls, and independent replication of a subset of the data [5,31]. Materials sourced from bovine products (e.g. bovine serum albumin) were avoided to remove the risk of contamination with *B. taurus* DNA, although the sequence differences between the two species over the region studied made the few contamination events easy to identify. A high-fidelity polymerase (Platinum Taq Hi-Fidelity, Invitrogen, UK) was used to reduce the polymerase error rate, and increase amplification efficiency [10,14,39]. The use of such enzymes enables sequence miscoding lesions to be confidently attributed to post-mortem DNA damage as opposed to errors introduced during enzymatic amplification [10]. PCR products were purified via precipitation using Microclean (Microzone, UK), and cloned using the Topo TA cloning system (Invitrogen, UK). Colonies were used to initiate PCR re-amplifications with vector M13R and T7 primers (Invitrogen, UK), purified as before, and sequenced on an ABI 3700 using the ABI Big Dye V3.1 PRISM kit (ABI Inc, USA).

```
1
CTACAGTCTC ACCGTCAACC CCCAAAGCTG AAGTTCTATT TAAACTATTC
51
CCTGAACGCT ATTAATATAG TTCCATAAAT GCAAAGAGCC TCACCAGTAT
101
TAAATTTACT AAAAATTCCA ATAACTCAAC ACAAATTTTG TACTCTAACC
151
AAATATTACA AACACCACTA GCTAACGTCA CTCACCCCCA AAATGCATTA
201
CCCAAATGGG GGGGACGTAC ATAATATTAA TGTAATAAAA ACATATTATG
251
TATATAGTAC ATTAAATTAT ATGCCCCATG CATATAAGCA AGTACTTAAT
301
CCCTATTGAT AGTACATAGT ACATAAAGTT ATTAATTGTA CATAGCACAT
351
TATGTCAAAT CTACCCTTGA CAACATGCAT ATCCCTTCCA TTAGATCACG
401
AGCTTAACTA CCATGCCGCG TGAAACCAGC AACCCGCTAG GCAGGGACCC
451
CTCTTCTCGC TCCGGGCCCA TGAATTGTGG GGGTCGCTAT TTAATGAACT
501
TTATCAGACA TCTGGTTCTT TCTTCAGGGC CATCTCATCT AAAATTGTCC
551
ATTCTTTCCT CTTAAATAAG ACATCTCGAT GGACTAATGG CTAATCAGCC
601
CATGCTCACA CATAACTGTG CTGTCATACA TTTGGTATTT TTTTATTTTG
651
GGGGATGCTT GGACTCAGCT ATGGCC
```

Fig. 1. *Bos bison* reference sequence (*BbRS*). As can be expected from their close evolutionary history, the *Bos bison* sequence bears close similarity to that of *Bos taurus*. For comparison, the first position of *BbRS* corresponds to position 15738 of *Bos taurus* Genbank sequence J01394 [14]. The *BbRS* contains these major modifications from the *Bos taurus* sequence (J01394): 15916/15917 AA deletion, 15921–15925 inclusive GCCCA deletion, 15927 A deletion, 15931–15933 inclusive AGA deletion, 15957 A deletion, 16058–16059 T insertion, 16121/16122 GT deletion, 16124–16126 inclusive TAT deletion, 16128 T deletion, 16133 T deletion, and 16143 A deletion.

2.1. Determination of site-specific post-mortem damage rates

Each PCR product was cloned, and the resulting individual clone sequences were aligned with the BbRS manually using the program SEQMAN 4.0 (DNAStar Inc). The consensus sequence for each PCR was determined from the specific nucleotide motifs shared between the majority of clones (for further details of this method see [12]). Any remaining base differences in the clones formed the post-mortem damage data set. The few base insertions and deletions (indels) observed were excluded from the analysis. Full details of the sequences are given in Shapiro et al. [31].

It is difficult to calculate site-specific post-mortem damage rates for a number of reasons [11]. A major problem is that when a set of clones derived from one PCR product share a pattern of damaged sites it is likely that they arose from the same ancestral template molecule, and therefore the number of times these damaged sites are observed will be proportional to the number of clones sequenced. Similarly, the number of undamaged starting templates is difficult to assess because they are better templates for amplification during the initial cycles than damaged templates. Furthermore, within a set of clones it is common to see jumping PCR spread damaged sites between daughter amplified strands, generating a few damaged sites at identical nucleotide sites between quite different sequences. Lastly, calculations are complicated because each section of the bison HVR sequence has been amplified and cloned a different number of times, making it difficult to compare rates between regions. Consequently, an approximate relative rate of post-mortem damage (ρ_v) was calculated for each site after Gilbert et al. [11], modified to account for the 9 HVR fragments that were amplified as part of the study (Table 2).

Table 1
Number of independent PCR amplifications over different portions of the bison control region

BbRS[a]	PCR[b]
21–37	8
38–66	15
67–92	16
93–166	19
167–184	17
185–261	23
262–272	20
273–289	7
290–292	6
293–308	8
309–341	10
342–349	9
350–416	6
417–419	17
420–434	30
435–496	29
497–560	24
561–616	22
617–642	16
643–657	3

[a] Position with reference to BbRS.
[b] Number of PCR amplifications covering region.

In this calculation, $\rho_v = \mu_v/\sigma_v$ where v = a specific site, μ_v = hits observed at a specific site across all sequences analyzed, and σ_v = total number of amplifications for each specific site. Due to the focus of the original bovid study, sequence positions occurring on the outer extremities of the HVR (between positions 24–272 and 417–679) have been more intensely studied, and therefore have a much larger denominator than those from the central region (positions 273–416). Consequently, to enable a meaningful comparison of damage rates and hotspots, we follow Gilbert et al. [11] and analyse two data sets (OR, outer region and MR, middle region) independently.

2.2. Hotspots

A null hypothesis (H_0) that post-mortem damaged sites were randomly distributed across each region (OR and MR) was tested through comparison with the modified expected Poisson distribution of Heyer et al. [17] utilised in Gilbert et al. [11]. The probability of sequence sites having exactly X substitutions, $P(X)$, is

$$P(X) = e^{-\lambda}\lambda^{X}/X!$$

Table 2
Rates of post-mortem DNA damage and inferred in vivo mutation at select sites within the 'MR' of the Bison Control Region

Site[a]	Mutation[b]	Damage[c]	*Bos taurus*[d]
273	2	3	b
293	0	0	a
300	34	0	a, c
301	32	1	a, b, c
308	39	0	a, b, c
309	4	0	a, c
318	9	0	a
320	1	0	a
321	0	2	a
326	0	1	a, c
331	0	0	a
337	44	0	a, c
340	2	1	a
347	0	0	a
361	8	0	a
365	29	2	a, c
373	0	0	c
380	0	0	b
383	1	3	a, c
384	1	2	a
386	3	0	a, b
390	0	0	a
408	39	6	a

[a] Bison Reference sequence position.
[b] In vivo mutation rate calculated as average number of homoplasies on two pairs of phylogenetic trees.
[c] Observed number of damage events.
[d] Sites identified as hotspots in three studies on *Bos taurus*. Studies are as follows: (a) TC99, Cymbron et al. [6]; (b) JW00, Wu et al. [40]; (c) CT01, Troy et al. [34].

where Poisson parameter λ refers to the observed density of mutations. To estimate the expected count, $LP(X)$, of sequence sites for each category, given the random distribution λ and the length L of the sequence, we multiply the Poisson probability $P(X)$ by the number of sequence sites L, such that

$$LP(X) = L\left(e^{-\lambda}\lambda^{x}/X!\right)$$

A chi-squared goodness of fit test can then be applied to the observed and expected results to determine whether the null hypothesis (H_0) of randomly distributed post-mortem damage can be rejected.

2.3. In vivo hotspots

To provide a comparison with the post-mortem damage spectrum, in vivo mutation rates for individual sites were calculated as the averages of values inferred from two pairs of mitochondrial genealogies generated from 172 bison sequences using Markov Chain Monte Carlo (MCMC) (Beth Shapiro, unpublished data). Four alternative tree topologies were used to ensure that a specific topology was not affecting rate estimates at individual sites. The trees represent the maximum aposteriori (MAP) and maximum likelihood (ML) estimates from two independent replicate MCMC analyses. Using the software MacClade (Sinauer Associates, MA, USA), the minimum number of mutations at each site, given each of the four fixed trees, was calculated. This maximum parsimony estimate is necessarily a lower limit of the number of changes at a given site, therefore it represents a conservative estimate of rate variation among sites, as fast evolving sites will typically have experienced many reversions in a large genealogy that are undetected by parsimony reconstruction.

Sites identified as hypervariable in three published studies of *B. taurus* mitochondrial DNA were also used for comparison. As the methods and data sets used to generate the data in each study were very different, the quantitative results are not directly comparable. Specifically, Wu et al. [40] use a familial method of real time observations, whereas Cymbron et al. [6] and Troy et al. [34] use phylogenetic methods. Therefore, individual sites were simply designated as being of hotspot or not-hotspot status.

3. Results

Six hundred and seventy-nine bison clones were analysed from 81 initial PCR reactions, producing 135,221 bases of mitochondrial DNA Light (L) strand data. There is strong evidence to suggest that the data do not derive from contamination. The sequences are drawn from a recently published study [31] that involved the generation of sequence data for, and subsequent phylogenetic analysis of, over 350 ancient bison. Several findings of that study argue for the authenticity of our data. Firstly, very few of the specimens from which DNA was obtained contained identical DNA sequences. Secondly, all the sequences were generated from multiple amplifications (on each individual DNA extract), and PCR products from over 200 of the bison extracts were cloned to check the authenticity of the sequences. Thirdly, the data from 76 of the samples was replicated on independent extracts. These three findings argue that cross-contamination of the extracts from other sources of DNA is unlikely – contamination would not have given the observed pattern of 'novel', replicable sequences yielded by each individual.

In addition to the above, there is enough sequence heterogeneity among the bison samples to ensure that the sequence of each particular sample contains an identifiable sequence 'motif' [31] that enables its differentiation from sequences derived from other samples (i.e., when their particular sequence is compared to a reference sequence, we observe particular mutations at particular positions). The subsequent damage

analyses involved scoring only that sequence variation observed in addition to these motifs. Therefore, as each 'damaged' sequence contains both the specimen-specific sequence motif plus the additional damage, it is unlikely that the sequence variation among the clones could arise from contamination. Should contamination have been the case, the motifs corresponding to the original sequence should have been absent in the contaminated sequence. For further details on this method refer to Ref. [12].

The spectra of observed damage types within the clones of the bison samples is 153/411(37.2%) Type 1 transitions, 244/411(59.4%) Type 2 transitions and only 14 other mutations. This overall bias towards transitions, and specifically towards the more biochemically likely Type 2 transitions [20,21] is as expected and has been seen in several other aDNA studies [10,14]. The distribution of Type 1 and Type 2 transitions amongst the clones from individual PCRs is similar, with both occurring as either singletons (occurring in only one or a few clones) or in multiple clones. The latter situation suggests that the source template existed at an early stage of the amplification process, spawning many daughter clones, and is therefore less likely to represent random polymerase error during amplification.

The spatial variation of post-mortem damage per site (calculated relative rate (ρ_n) of post-mortem damage) and homoplasies per site calculated for the bison data set can be seen in Figs. 2 and 3. Almost no variation was observed in the rates of mutation calculated for individual sites between the different topologies, so the average values per site closely match those calculated from each tree. The variation of post-mortem damage appears to be over-dispersed with certain sites over represented, notably BbRS sites 273, 303, 312, 313, 383, 400, 408, 411 and 412. The null hypothesis (H_0) of random post-mortem damage distribution can be strongly rejected for the MR (χ^2, $p < 0.00$), though not for the OR, $p = 0.2038$), demonstrating that at least in the MR sites are not being damaged at random. Similarly, a random distribution of homoplasies in the modern data set can also be rejected ($p < 0.00$).

The broad range of damage (0–48) and mutation rate (0–6) measurements make direct comparison difficult, but the majority of sites within the bison control region with low rates of post-mortem damage also have low in vivo mutation rates. However, as for ancient human mtDNA sequences, we observe some disagreement. In particular, at least 15/144 sites within the MR have obviously conflicting rates, where sites with high values in one data set (measured as over half of the maximum rate observed) were associated with rates of zero in the other data set. However, it should be noted that this disagreement is not only between the damage and mutational data sets, but also between the location of mutational hotspots identified here and previously (Table 2). Full details of site mutation and damage rates are given in Supplementary data.

4. Discussion

The spectrum of damage within cloned ancient bison sequences is consistent with previous studies of aDNA

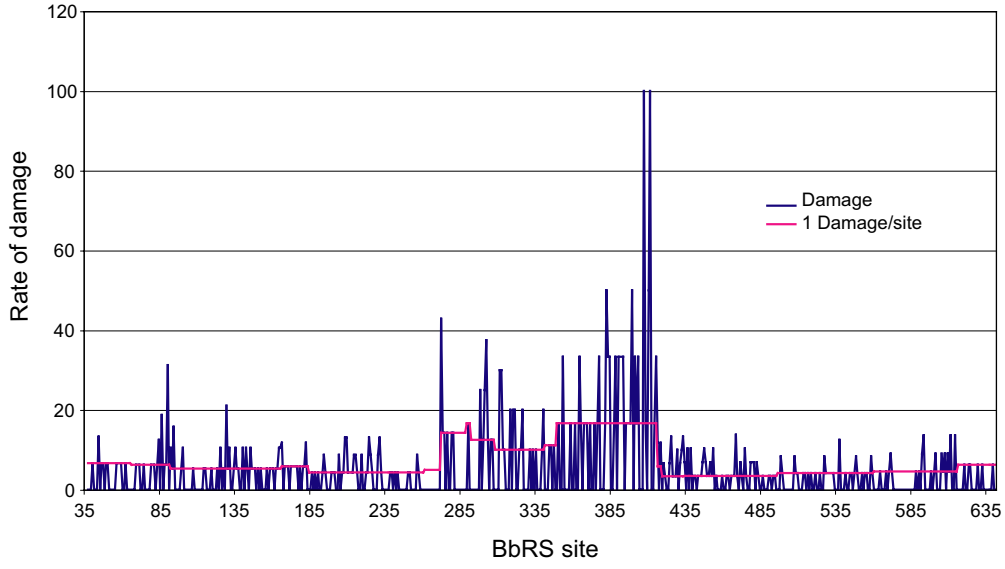

Fig. 2. Variation of relative damage rate across *Bos bison* mtDNA Control Region. Variation in relative damage rate across the bison control region, from positions 24 to 269 of the *Bison bison* reference sequence (*BbRS*). The relative rate calculations are described in the text. The level of 'resolution' at each site is indicated by underlying grey line (pink line in online version). Differences in 'resolution' arise due to the fact that particular sites have undergone different numbers of PCR amplifications in the study. Thus, as relative damage rates are normalised for numbers of PCRs, the minimum relative rate that could be observed for a particular site (grey line) will depend on this initial number of PCRs.

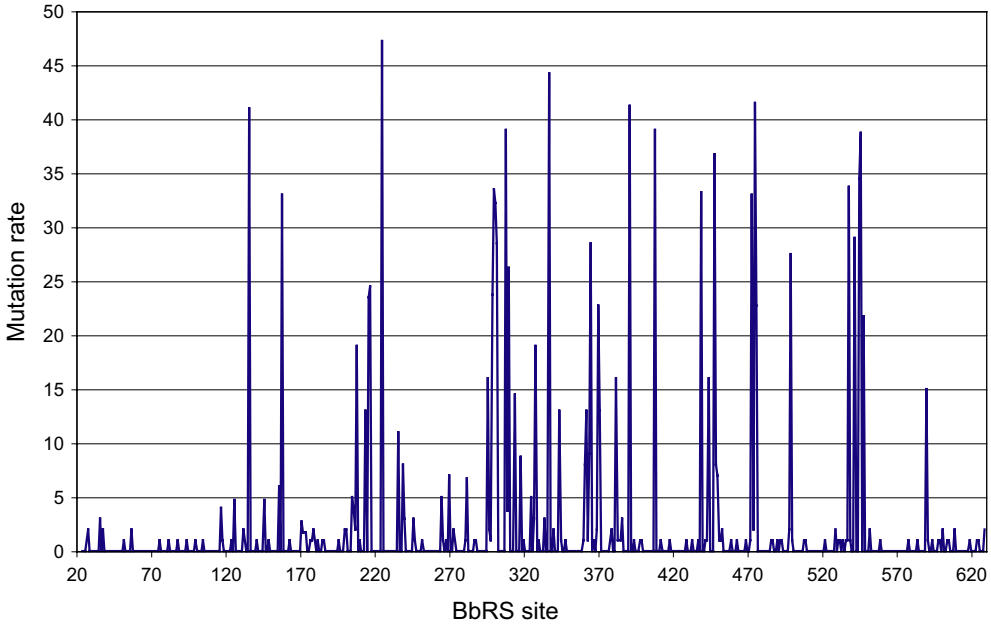

Fig. 3. Variation of estimated mutation rate across *Bos bison* mtDNA Control Region. Estimates of the in vivo mutation rates per site across the bison control region.

damage [10,18], and shows strong evidence for post-mortem damage hotspots in at least part of the bison control region. Although there is no statistical evidence to support the existence of such hotspots in the OR, several sites appear to receive a disproportionate amount of the damage, such as BbRS sites 91 and 130.

In agreement with previous studies of ancient human sequences, the majority of sites exhibit similar properties of post-mortem damage and in vivo mutation, suggesting mutational hotspots exist within both human and non-human sequences, and that these are not artefacts of sample contamination or recombination [10]. The bovid and human data sets are also similar in having a number of sites with divergent mutation and damage rate estimates. These discrepancies are not only seen between the post-mortem and mutational data sets generated in this study, but also between both of these and hotspots identified in previous studies of bovid sequences [6,34,40]. A proportion of these inconsistencies may result from sampling stochasticity, however, since this pattern is also common among studies of modern human mutation rates [3], it is probable that much of the discrepancy is due to the phylogenetic models used for the estimation of mutation rates. Of course, it is also likely that the processes leading to mutation in vivo and miscoding lesions post-mortem are somewhat qualitatively different.

The secondary structure of mitochondrial DNA has been suggested to influence the susceptibility of sites to damage events [25], and this may explain the similarity between post-mortem and in vivo rates for HVR1. However, mutation rates for sequences with functional roles in vivo will be a product of both structural constraints and selection, and therefore should differ markedly from post-mortem rates. Indeed, this pattern has been observed in both human mitochondrial COIII sequences and the functional HVR1 elements ETAS and Mt5 [11]. If in the future similar structural elements can be determined in the bison control region, it will naturally be interesting to examine whether similar patterns exist.

An understanding of the selection pressures acting on supposedly neutral DNA sequences (such as the mitochondrial control region) has important implications for both evolutionary studies and phylogenetic reconstruction, in particular with regards to the development of the models of molecular evolution that so often underpin the analyses. In addition, the presence of post-mortem damage hotspots that correlate with in vivo mutational hotspots also has more direct implications for aDNA studies. As discussed previously [11], a serious risk exists that DNA sequences retrieved from uncloned and/or unreplicated aDNA extractions will be modified in such a way as to contain erroneous phylogenetic information.

Acknowledgements

The authors would like to thank Hendrik Poinar, Hans-Jurgen Bandelt and Mike Bunce for useful discussion. Partial financial support was provided by the Wellcome Trust (MTPG, AC), Rhodes Trust (BS), Leverhulme Trust (AC), NERC (AC, BS), and BBSRC (AD).

Appendix A. Supplementary information

Supplementary information detailing the complete distribution of post-mortem damage and in vivo mutations across the bison Control Region can be found, in the online version, at doi:10.1016/j.jas.2005.02.006.

References

[1] S. Anderson, M.H.L. De Bruijn, A.R. Coulson, E.C. Eperon, F. Sanger, I.G. Young, Complete sequence of bovine mitochondrial DNA, J. Mol. Biol. 156 (1982) 683–717.

[2] S. Aris-Brisou, L. Excoffier, The impact of population expansion and mutation rate heterogeneity on DNA sequence polymorphism, Mol. Biol. Evol. 13 (1996) 494–504.

[3] H.-J. Bandelt, L. Quintana-Murci, A. Salas, V. Macaulay, The fingerprint of phantom mutations in mitochondrial DNA data, Am. J. Hum. Genet. 71 (2002) 1150–1160.

[4] K.E.V. Bendall, V.A. Macaulay, J.R. Baker, B.C. Sykes, Heteroplasmic point mutations in the human mtDNA Control Region, Am. J. Hum. Genet. 59 (1996) 1276–1287.

[5] A. Cooper, H. Poinar, Ancient DNA: do it right or not at all, Science 289 (2000) 1139.

[6] T. Cymbron, R.T. Loftus, M.I. Malheiro, D.G. Bradley, Mitochondrial sequence variation suggest an African influence in Portuguese cattle, Proc. R. Soc. Lond. B 266 (1999) 597–603.

[7] L. Excoffier, Z. Yang, Substitution rate variation among sites in mitochondrial hypervariable region I of humans and chimpanzees, Mol. Biol. Evol. 16 (1999) 1357–1368.

[8] S. Finnilä, M. Lehtonen, K. Majamaa, Phylogenetic network for European mtDNA, Am. J. Hum. Genet. 68 (2001) 1475–1484.

[9] L. Forster, P. Forster, S. Lutz-Bonengel, H. Willkomm, B. Brinkmann, Natural radioactivity and human mitochondrial DNA mutations, Proc. Natl Acad. Sci. U.S.A. 99 (2002) 13950–13954.

[10] M.T.P. Gilbert, A.J. Hansen, E. Willerslev, L. Rudbeck, I. Barnes, N. Lynnerup, A. Cooper, Characterisation of genetic miscoding lesions caused by post mortem damage, Am. J. Hum. Genet. 72 (2003) 48–61.

[11] M.T.P. Gilbert, E. Willerslev, A.J. Hansen, L. Rudbeck, I. Barnes, N. Lynnerup, A. Cooper, Distribution patterns of post mortem damage in human mitochondrial DNA, Am. J. Hum. Genet. 72 (2003) 32–47.

[12] M.T.P. Gilbert, L. Rudbeck, E. Willerslev, A.J. Hansen, C. Smith, K.E.H. Penkman, K. Prangenberg, C.M. Nielsen-Marsh, M.M.E. Jans, P. Arthur, N. Lynnerup, G. Turner-Walker, M. Biddle, B. Kjølbye-Biddle, M. Collins, Biochemical and physical correlates of DNA contamination in archaeological human bones and teeth excavated at Matera, Italy, J. Archaeol. Sci. 32 (2005) 785–793.

[13] E. Hagelberg, Recombination of mutation rate heterogeneity? Implications for Mitochondrial Eve, Trends Genet. 19 (2003) 84–90.

[14] A. Hansen, E. Willerslev, C. Wiuf, T. Mourier, P. Arctander, Statistical evidence for miscoding lesions in ancient DNA templates, Mol. Biol. Evol. 18 (2001) 262–265.

[15] M. Hasegawa, A. Di Rienzo, T. Kocher, A. Wilson, Towards a more accurate time scale for the human mitochondrial gene tree, J. Mol. Evol. 37 (1993) 347–354.

[16] M. Hasegawa, S. Horai, Time of the deepest root for polymorphism in human mitochondrial DNA, J. Mol. Evol. 32 (1991) 37–42.

[17] E. Heyer, E. Zietkiewicz, A. Rochowski, V. Yotova, J. Puymirat, D. Labuda, Phylogenetic and familial estimates of mitochondrial substitution rates: study of control region mutations in deep-rooting pedigrees, Am. J. Hum. Genet. 69 (2001) 1113–1126.

[18] M. Hofreiter, V. Jaenicke, D. Serre, A. von Haeseler, S. Pääbo, DNA sequences from multiple amplifications reveal artefacts induced by cytosine deamination in ancient DNA, Nucleic Acids Res. 29 (2001) 4793–4799.

[19] N. Howell, C.B. Smejkal, D.A. Mackay, P.F. Chinnery, D.M. Turnbull, C. Herrnstadt, The pedigree rate of sequence divergence in the human mitochondrial genome: there is a difference between phylogenetic and pedigree rates, Am. J. Hum. Genet. 72 (2003) 659–670.

[20] P. Karran, T. Lindahl, Hypoxanthine in deoxyribonucleic acid: generation by heat-induced hydrolysis of adenine residues and release in free form by a deoxyribonucleic acid glycosylase from calf thymus, Biochemistry 19 (1980) 6005–6011.

[21] T. Lindahl, DNA glycosylases, endonucleases for apurinic/apyrimidinic sites and base excision-repair, Prog. Nucleic Acid Res. Mol. Biol. 22 (1979) 135–192.

[22] V. Macaulay, M. Richards, P. Forster, K. Bendall, E. Watson, B. Sykes, H.-J. Bandelt, mtDNA mutation rates – no need to panic, Am. J. Hum. Genet. 61 (1997) 983–986.

[23] B.A. Malyarchuk, I.B. Rogozin, V.B. Berikov, M.V. Derenko, Analysis of phylogenetically reconstructed mutational spectra in human mitochondrial DNA control region, Hum. Genet. 111 (2002) 46–53.

[24] S. Meyer, A. von Haeseler, Identifying site-specific substitution rates, Mol. Biol. Evol. 20 (2003) 182–189.

[25] S. Meyer, G. Weiss, A. von Haeseler, Pattern of nucleotide substitution and rate heterogeneity in the hypervariable regions I and II of human mtDNA, Genetics 152 (1999) 1103–1110.

[26] S. Mumm, M.P. Whyte, R.V. Thakker, K.H. Buetow, D. Schlessinger, mtDNA analysis shows common ancestry in two kindreds with X-linked recessive hypoparathyroidism and reveals a heteroplasmic silent mutation, Am. J. Hum. Genet. 60 (1997) 153–159.

[27] S. Pääbo, Ancient DNA: extraction, characterisation, molecular cloning and enzymatic amplification, Proc. Natl Acad. Sci. U.S.A. 86 (1989) 1939–1943.

[28] S. Pääbo, D. Irwin, A. Wilson, DNA damage promotes jumping between templates during enzymatic amplification, J. Biol. Chem. 265 (1990) 4718–4721.

[29] T.J. Parsons, D.S. Muciec, K. Sullivan, N. Woodyatt, R. Alliston-Greiner, M.R. Wilson, D.L. Berry, K.A. Holland, V.W. Weedn, P. Gill, M.M. Holland, A high observed substitution rate in the human mitochondrial DNA control region, Nat. Genet. 15 (1997) 363–368.

[30] G. Pesole, C. Saccone, A novel method for estimating substitution rate variation among sites in a large dataset of homologous DNA sequences, Genetics 157 (2001) 859–865.

[31] B. Shapiro, A.J. Drummond, A. Rambaut, M.C. Wilson, P. Matheus, A.V. Sher, O.G. Pybus, M.T.P. Gilbert, I. Barnes, J. Binladen, E. Willerslev, A.J. Hansen, D.F. Baryshnikov, J.A. Burns, S. Davydov, J.C. Driver, D. Froese, C.R. Harington, G. Keddie, P. Kosintsev, M.L. Kuntz, L.D. Martin, R.O. Stephenson, J. Storer, R. Tedford, S. Zimov, A. Cooper, Rise and fall of the Beringian steppe bison, Science 306 (2004) 1561–1565.

[32] S. Sigurðardóttir, A. Helgason, J.R. Gulcher, K. Stefansson, P. Donnelly, The mutation rate in the human mtDNA control region, Am. J. Hum. Genet. 66 (2000) 1599–1609.

[33] M. Stoneking, Hypervariable sites in the mtDNA control region are mutational hotspots, Am. J. Hum. Genet. 67 (2000) 1029–1032.

[34] C.S. Troy, D.E. MacHugh, J.F. Bailey, D.A. Magee, R.T. Loftus, P. Cunningham, A.T. Chamberlain, B.C. Sykes, D.G. Bradley, Genetic evidence for Near-Eastern origins of European cattle, Nature 410 (2001) 1088–1091.

[35] Y. Van de Peer, J.M. Neefs, P.D. Rijk, R.D. Wachter, Reconstructing evolution from eukaryotic small-ribosomal-subunit RNA sequences: calibration of the molecular clock, J. Mol. Evol. 37 (1993) 613–623.
[36] Y. Van de Peer, S.L. Baldauf, W.F. Doolittle, A. Meyer, An updated and comprehensive rRNA phylogeny of (crown) eukaryotes based on rate-calibrated evolutionary distances, J. Mol. Evol. 51 (2000) 565–576.
[37] L. Vigilant, M. Stoneking, H. Harpending, K. Hawkes, A.C. Wilson, African populations and the evolution of human mitochondrial DNA, Science 253 (1993) 1503–1507.
[38] J. Wakely, Substitution rate variation among sites in hypervariable region I of human mitochondrial DNA, J. Mol. Evol. 37 (1993) 613–623.
[39] E. Willerslev, A.J. Hansen, B. Christensen, J. Steffensen, P. Arctander, Diversity of Holocene life forms in fossil glacier ice, Proc. Natl Acad. Sci. U.S.A. 96 (1999) 8017–8021.
[40] J. Wu, R.K. Smith, A.E. Freeman, D.C. Beitz, B.T. McDaniel, G.L. Lindberg, Sequence heteroplasmy of D-loop and rRNA coding regions in mitochondrial DNA from Holstein cows of independent maternal lineages, Biochem. Genet. 38 (2000) 323–335.